

Complex geophysical investigation of the Kapušany landslide (Eastern Slovakia)

David KUŠNIRÁK, Ivan DOSTÁL, René PUTIŠKA, Andrej MOJZEŠ

Department of Applied and Environmental Geophysics, Faculty of Natural Sciences, Comenius University, Mlynská dolina, Ilkovičova 6, 842 48 Bratislava, Slovak Republic; e-mail: kusnirak@fns.uniba.sk; dostal@fns.uniba.sk; putiska@fns.uniba.sk; mojzes@fns.uniba.sk

Abstract: Geophysical survey is a very useful and popular tool used by engineering geologists to examine landslides. We present a case study from the Kapušany landslide, Eastern Slovakia, where a broad spectrum of geophysical methods were applied along two perpendicular profiles in order to compare the ability of the methods to detect as many structural features of the landslide as possible. The 2D Electrical Resistivity Tomography inverse model was capable of defining the geological structure of the landslide and defining the shear zone, however the resolution of the inverse model does not allow us to identify cracks or other minor features of the landslide. These, however, were well recorded in the results of Dipole Electromagnetic Imaging and the Self Potential method. In addition microgravimetry, Gamma-Ray Spectrometry and Soil Radon Emanometry were experimentally employed to validate the results obtained from electrical methods and afterwards final geological models, based on the integrated interpretation of all involved methods were constructed.

Key words: near-surface geophysics, landslide, shear zone, Kapušany, Eastern Slovakia

1. Introduction

Landslides of various sizes and types are a very widespread form of slope deformation and represent a serious hazard in urban areas (*Hungr et al., 2014*). Geophysical survey methods help to locate landslide areas, especially in identifying potential landslides, but also in monitoring landslide bodies after activation (*Prokešová et al., 2014*). Within the scope of the project “Diagnosis of landslides using modern geophysical and engineering geological approaches” we used several geophysical methods to define landslides in geophysical fields. For testing the following methods were used:

Electrical Resistivity Tomography (ERT), Dipole Electromagnetic Imaging (EMI), Self Potential (SP), Gamma-Ray Spectrometry (GRS) and Soil Radon Emanometry (SRE) and microgravimetry. The test site is located in the village of Kapušany in eastern Slovakia (Fig. 1). In May 2010, there was an activation of a landslide below individual houses due to extreme rainfall with a monthly cumulative total of 193.0 mm. As a result of slope movements 11 houses were damaged and 7 of them had to be demolished. The aim of our test on this area was to find out the impact of individual structural parts of the landslide on the observed geophysical fields. Additionally, comparing results of different geophysical methods we try to pinpoint the pros and cons of the involved methods and to create an integrated final 2D model. The motivation to prepare cross-correlated and reliable geological-

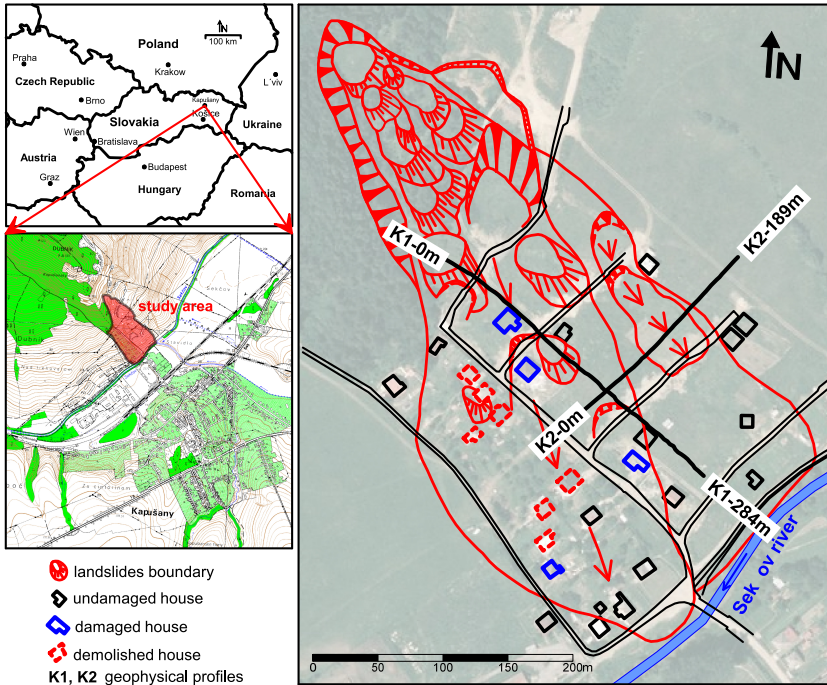


Fig. 1. Situation map of the Kapušany landslide. Actual position of the geophysical profiles K1 and K2 are shown as black lines, the activated landslide body is outlined by red lines.

geophysical models in landslide areas is also to increase the information value for the other cooperating geoscientists. These models can also serve as reference models for long term landslide monitoring using modern geophysical and engineering geological approaches.

The Kapušany landslide is located in the north-western part of the village of Kapušany in the eastern part of Slovakia (Fig. 1). The actual landslide body is located on the southeast oriented slope beneath Kapušany Castle. Three stages of engineering-geological survey were carried out within the study area. These included a number of drilling works (*Čermák and Varga, 1999; Grech, 2010; Laffers et al., 2012*). The activated landslide area (*Grech, 2010*) is approximately 500 m long and 200 m wide (Fig. 1). The landslide stream contains smaller sub landslides, in the upper part usually having a block character, while in the middle and bottom parts they are formed by several debrisflows. The area of interest is composed of Palaeogene sedimentary rocks, Neogene volcanic rocks and Quaternary sediments. Flysch type sediments of Palaeogene age are composed of layered sandstones, claystones and siltstones. Pyroxene-amphibolite bearing andesites represent the prevailing volcanic rock type in the study area. Quaternary sediments in the upper part of the landslide body are composed of rock and earth debris with fragments of andesite. In the lower part of the landslide body there are mainly clays with fragments of weathered bedrock. The main part of the landslide body is composed of fine grained soils of various gradimetric composition (*Grech, 2010*).

2. Methods

Geophysical measurements of this site were done on two profiles K1 to K2 (Fig. 1). The profiles are placed perpendicularly to each other, whereas the direction of profile K1 is parallel to the direction of landslide movement and profile K2 is placed across the landslide body. We carried out measurements of ERT, EMI, GRS and SRE on both profiles, gravity and SP measurements were done only on the K1 profile. All the geophysical methods were accurately positioned with a GNSS Trimble GeoExplorer 6000 Series GeoXR equipment in Real Time Kinematic (RTK) mode. RTK measurements were realized using the Slovak official positioning service SKPOS in Virtual Reference Station (VRS) concept.

2.1. Electrical Resistivity Tomography

Geoelectrical imaging techniques such as ERT are widely used for studying environmental and engineering problems (*Pellerin, 2002*). The ERT produces spatial or volumetric models of subsurface resistivity distributions, from which features of contrasting resistivity may be located and characterized. Methodologies for 2D and 3D ERT data collection and modelling are described, for example, by *Dahlin et al. (2002)* and *Lapenna et al. (2005)*.

Most rocks conduct electricity mainly by the movement of ions in pore water. Porosity and pore water composition are the major factors that control the resistivity of rocks. Due to the presence of water, the electrical conductivity of unconsolidated displaced material of a landslide would normally be higher than in the non-sliding material. The conductivity of the sliding material will also be increased if circulation water is highly mineralized or if it includes clay (*Bruno and Marillier, 2000*). Therefore, methods that detect changes in subsurface electrical properties can be useful for detecting and mapping the rupture surface of a landslide (*Goryainov et al., 1988; Grandjean et al., 2011*). For this purpose we employed ERT and EMI method to reconstruct the subsurface resistivity distribution.

The ERT measurements have been performed using the ARES II equipment (GF Instruments Inc., Brno, Czech Republic). The dipole-dipole and Wenner-Alpha electrode array with 3 m electrode distance were used. For post-processing and data interpretation, the inversion program RES2DINV (*Loke and Barker, 1996*) was applied. As an input for the inversion a collocated dataset from both field datasets was created. A standard least-squares constraint inversion (L_2 norm) with topography was used because it gives optimal results where subsurface geology exhibits a smooth variation, such as the shear zone shape (*Dostál et al., 2014*).

2.2. Dipole Electromagnetic Imaging

The EMI measurements were made at discrete points (station separation 3 m) with CMD Explorer equipment (GF Instruments Inc., Brno, Czech Republic) with three receiving coils and effective depths of 2.2, 4.2 and 6.7 m. The acquired apparent resistivity readings were filtered for outliers and used directly for interpretation.

2.3. Self Potential

The self-potential method (SP) involves the passive measurement of the electrical potential distribution at the ground surface of the Earth with non-polarizable electrodes. This method maps the electrical potential associated with different charge polarization mechanisms occurring at depth. These mechanisms can be due to an electrokinetic coupling (*Birch, 1998; Rizzo et al., 2004*), electrochemical coupling like diffusion of ionic species (*Maineult et al., 2004*), oxide-reduction reactions in the case of contaminants (*Naudet et al., 2004*) or ore deposits (*Corry, 1985*); and thermoelectric coupling (*Di Maio et al., 1998; Finizola et al., 2004*). As concerns the landslide, the main source of the SP signal is usually associated with groundwater flow through the electrokinetic coupling. This phenomenon is controlled by the relative motion between the charged mineral surface (negative in siliceous minerals such as clays) and the excess of charges located in the electrical diffuse layer of the pore fluid (*Lorne et al., 1999; Revil et al., 1999*). In this scheme, positive charges are carried out in the direction of the fluid flow, producing positive SP anomalies on the surface where water discharge is located and negative SP anomalies in the sites of infiltration. This hydro-electrical conversion can be detected by SP surveys and can allow zoning of infiltration water recharge and runoff areas.

SP method was applied in the fixed-based configuration with non-polarizable electrodes (Cu/CuSO₄). The step of measurements was again every 3 m and at every station the potential reading was repeated 3–5 times to ensure the correct measurement and to eliminate noise. The readings were afterwards averaged for every station and the measured values were corrected by the value of polarization of the electrodes.

2.4. Microgravimetry

Application of microgravimetry measurement for landslide characterization is rare nowadays. The current level of instrumentation allows us, assuming good knowledge of morphological features of the terrain in question, to detect not only basic geological structures but also to characterize changes in porosity or in jointing. The application of gravity measurements in the monitoring of landslide areas, particularly in the period of expected (potential) increase in the slope activities can be considered highly promising (*Bárta*

et al., 2005). Gravity measurements on the profile K1 were done using the station separation of 6 m, between the 100 and 210 of profile length the station separation was decreased to 3 m. An instrument used for the data acquisition was Scintrex CG-5 gravity meter with a measurement cycle time of 60 seconds at every station. A total number of 64 gravity readings were processed to remove instrument drift, which was determined by repetitive measurement at the base station located on a concrete plate close to the centre of the profile over a period of 1 hour and afterwards processed into form of complete Bouguer anomaly (e.g. *Reynolds*, 2011).

2.5. Gamma-Ray Spectrometry

It is supposed that the mineralogical and chemical composition of weathering and soil cover is rather monotonous and uniform as the studied landslide area is not large. Therefore, the changes of total gamma activity eUt values are assigned to the variability of clay content in cover (*Ruffell and Wilson*, 1998). This way, the profile parts of higher eUt values determine some quasi-homogeneous blocks of more consolidated rock material (slide bodies and stable areas) with higher clay content while the parts with lower eUt values rather indicate the edges of uniform blocks where the rock material is less consolidated, reworked by movement, with lower clay content as the result of washing by precipitation and de-arrangement of particles (*Mojzeš*, 2000b). The GRS measurements were done along both profiles K1 and K2 with 2 or 3 m step between stations. Totally, 192 stations were measured, each one of 100 or 120 s of accumulation time. The obtained concentrations of ^{40}K , ^{238}U and ^{232}Th radioisotopes were converted to the total gamma activity eU_t [Ur] (1 Ur \sim 1 ppm eU). A portable gamma-ray spectrometer GS-256 (producer Geofyzika, State Company, Brno, former Czechoslovakia) with scintillation detector NaI (Tl) 76×76 mm and 256-channel analyser was used for measurements.

2.6 Soil Radon Emanometry

It is also supposed that the studied landslide did not originate from deep based tectonics. Therefore, the values of soil ^{222}Rn volume activity $a_{V,222\text{Rn}}$ are basically derived from local mineralogical and petrophysical composition

of weathering cover (Ramola *et al.*, 2008). In this way, analogically to the gamma-ray spectrometric results, the higher values of $a_{V,222Rn}$ are attributed to quasi-homogeneous consolidated rock blocks and the lower ones to zones of less consolidated, loosened and more permeable material where soil radon gas can escape from soil into the atmosphere (Mojzeš, 2000a; Gajdoš *et al.*, 2002). The SRE measurements were done along the whole K1 profile and between 0 to 120 m stations on the K2 profile with 1 to 5 m (mostly 3 m) station separation. Totally, 133 stations were measured. Soil air was sampled from the depth of 0.8 m and volume activity of radon isotope ^{222}Rn $a_{V,222Rn}$ [kBq m⁻³] was determined in the air sample. A portable radon detector LUK-3R (producer SMM Inc., Prague, Czech Republic) working on the basis of exchangeable Lucas scintillation ZnS(Ag) cells, was used for measurements.

3. Results and Discussion

The geophysical survey of the Kapušany landslide was performed in October 2014, when the morphological features of the active part of the landslide were no longer visible on the ground. The integrated interpretation of all used geophysical methods on profiles K1 and K2 allows us to identify minor structural features of the main landslide body (cracks relicts A1–A5; minor earth slides B1–B4), in addition to the main features such as the shear zone, main scarp and lateral landslide extents (Figs 2, 3). This contribution is focused on the minor landslide features assessment, which are better visible on the profile K1 situated parallel to the landslide movement (Fig. 1).

The results of radiometric measurements presented in Figures 2a and 3a do not fully satisfy the theoretical expectations explained in the previous chapter. Local maxima of eU_t and $a_{V,222Rn}$ curves fit quite acceptably with the positions of minor earth slides (B1–B3 on the K1 profile) and stable areas on both profiles while their local minima corresponding to zones of crack relicts (A1 and A2 and possibly another around 160–170 m on the K1 profile), landslide edges and asphalt roads on both profiles.

There are several special parts with different origins of anomalies: the highest eU_t anomaly (up to 22 Ur) and the minimal $a_{V,222Rn}$ values between positions $x = 220–240$ m on the K1 profile are caused by artificial material and technology (ground isolation) used for building foundations. The

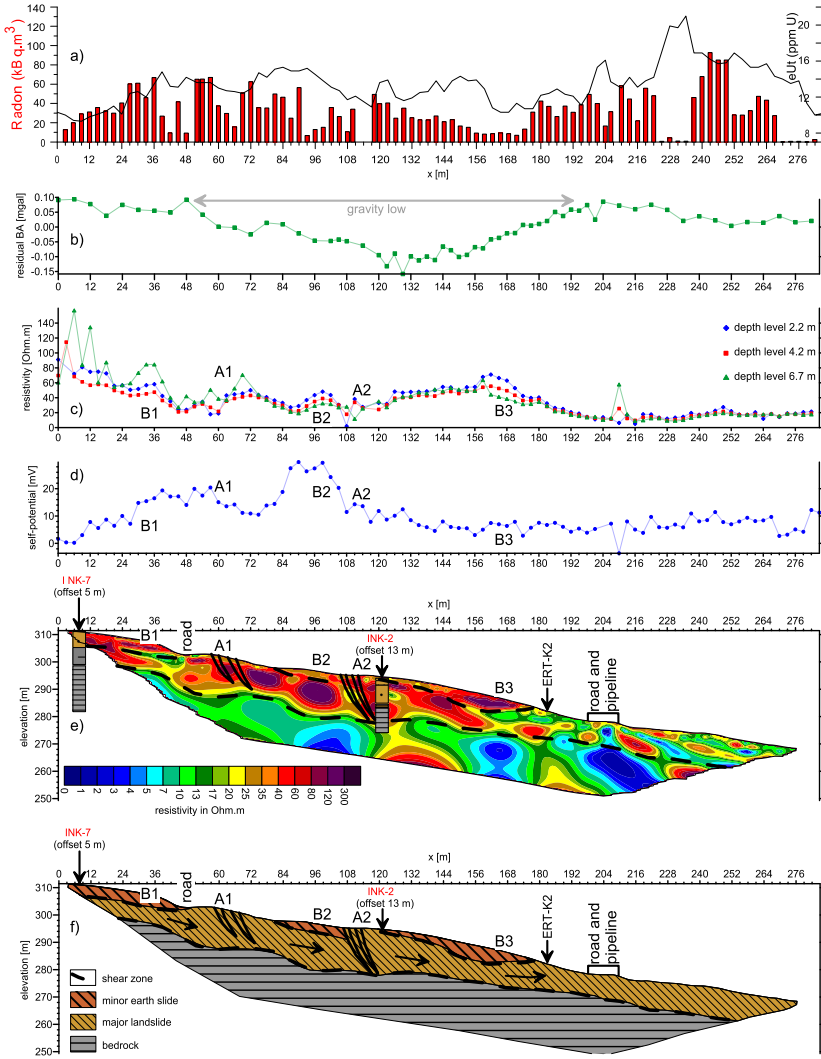


Fig. 2. Results of geophysical measurements on profile K1 with mark-up of the identified landslide structural features – shear zone, crack relicts (A1–A2) and minor earth slides (B1–B3). a) Volume activity of radon isotope ^{222}Rn (red bars) and total gamma activity $e\text{U}\text{t}$ (black line); b) Observed residual Bouguer anomaly; c) Apparent resistivity values measured by the EMI method in different depth levels; d) Self-potential field obtained in fixed-based electrode configuration; e) Inverse model resistivity cross-section; f) Geological model, based on the integrated interpretation of all involved methods (a–e).

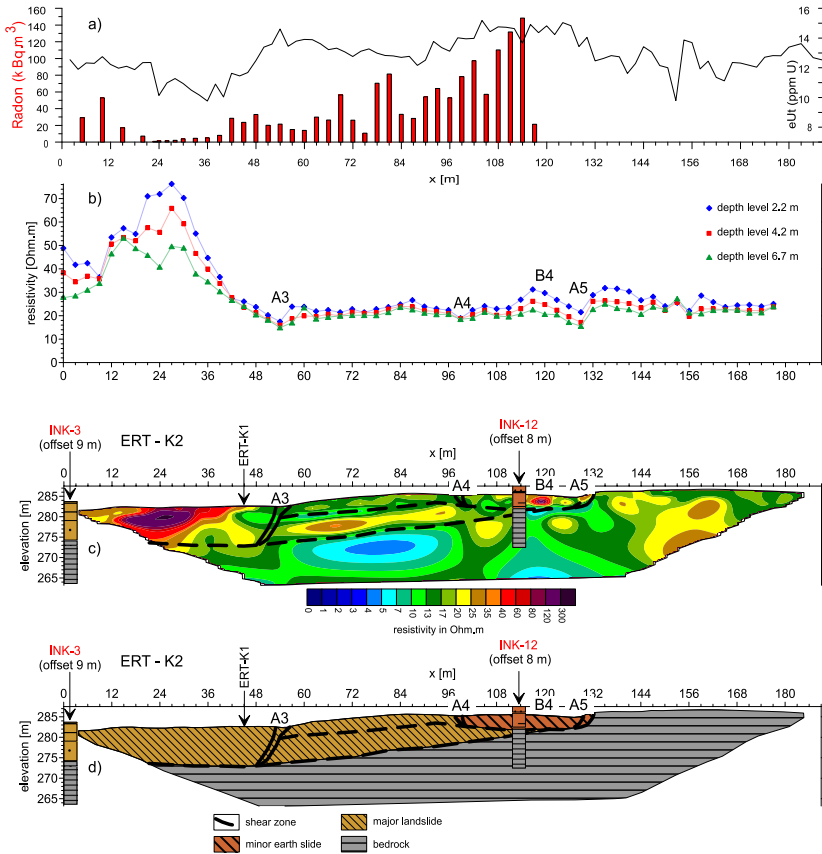


Fig. 3. Results of geophysical measurements on profile K2 with mark-up of the identified landslide structural features – shear zone, crack relicts (A3-A5) and minor earth slide (B4). a) Volume activity of radon isotope ^{222}Rn (red bars) and total gamma activity eU_t (black line); b) Apparent resistivity values measured by the EMI method at different depth levels; c) Inverse model resistivity cross-section; d) Schematic geological model, based on the integrated interpretation of all involved methods (a-c).

minimal $a_{V,^{222}Rn}$ values and rapidly decreasing eU_t values at the end of the K1 profile (located at $x = 265–285$ m) are caused by a waterlogged zone. Low eU_t and $a_{V,^{222}Rn}$ values between 20–40 m on the K2 profile show good correlation with EMI results and indicate the presence of a shallow near-surface compact rock body.

The shape of the Bouguer gravity curve between the 50 m and 190 m correlates well with the definition of the main body of the landslide (Fig. 2b). Minima in the curve are due to a decrease of the bulk density within the main landslide body as a result of the disintegration of the redeposited sediments. Total amplitude of the low gravity anomaly is 0.25 mGal and width of the anomaly is 156 m (located at $x = 48–204$ m on profile K1).

The EMI method provides information about the resistivity of the ground only in the near-surface zones, and responds primarily to the presence of the pull-off zones, which can be identified in the data as a sudden drop in the measured resistivity values – anomalies A1 and A2 on profile K1 (Fig. 2c) and A3–A5 on profile K2 (Fig. 3b). Accumulation zones of minor earth slides B1–B3 on profile K1 (Fig. 2c) and B4 on profile K2 (Fig. 3b) can be identified in the resistivity curves as differentiated values for each specific depth.

In the SP field (Fig. 2d), the crack relict areas A1 and A2 appear as a reduced value of the measured potential – surface water infiltration zone. The position of the anomalies in the SP field correlates well with the EMI results, where the resistivity image shows that the infiltration zones are characterized by lower resistivity values. The observed drop in the resistivity is most likely caused by increased water content in the infiltration zone. Minor earth slides B1–B2 are presented as an increase of the measured self-potential values, caused by water accumulating in the landslide body. This explanation is not applicable for the zone B3, which indicates continuous ground water flow into the main landslide body.

The main landslide body on profile K1 can be identified in the ERT inverse model (Fig. 2e) as an increased resistivity zone at a depth of about 15 m in the upper part of the profile ($x = 0–180$ m), whereas the rest of the profile indicates low resistivity contrast between the main landslide body and bedrock. The change in the resistivity image is related to the different composition of the landslide body, whereas the upper part is built by earth debris with fragments of andesite and the lower part is composed mainly by clays with fragments of weathered bedrock. The bedrock is formed by alternating sandstones and clays with slightly lower resistivity values (1–20 Ω m). The shear zone was interpreted in the inverse model based on main two constraints – 1) identified shear zone in boreholes INK-7 and INK-2 (Grech, 2010); 2) following the 20 Ω m isoline in the inverse model

(Fig. 2e and 2f). On profile K2, which is orientated across the main landslide body, the interpretation of the shear zone was performed in the same manner as for profile K1, where the involved boreholes were INK-3 and INK-12 described by *Grech (2010)*. The observed resistivity range 15–40 Ω m in the near-surface zone indicates landslide material composition described for the lower part of the landslide body. The spatial extent of the main body is defined by the A5 anomaly on position $x \approx 130$ m. Resolution of both calculated inverse models cannot reliably identify crack relicts A1–A5, however the minor earth slides B1–B4 can be clearly differentiated from the main landslide body, regarding the increased resistivity of these features.

4. Conclusions

Based on integration of the partial results and interpretations of all involved geophysical methods applied along two perpendicular profiles K1 and K2 in the Kapušany Landslide schematic geological models were compiled (Fig. 2f and Fig. 3d respectively). The major information concerning the internal structure of the landslide body was adopted from the Electrical Resistivity Tomography (ERT) inverse model, specifically the shear zone delineation and minor earth slides definition. However the minor features, which are the main objective of this contribution, could be overseen in this model. Therefore additional methods – self-potential (SP), electromagnetic imaging (EMI), microgravity, Gamma-Ray Spectrometry (GRS) and Soil Radon Emanometry (SRE) were essential to gather a broad spectrum of knowledge about the internal structures and mechanisms of the investigated landslide. The application of the SRE and GRS methods for this study contributed to the overall concept only marginally. The correlation of the SRE and GRS results with other involved geophysical methods is rather low, however on the K2 profile the observed minima in SRE and GRS corresponds to the near surface highly resistive body. Very satisfying results were obtained from the electromagnetic imaging, where the measured resistivity field helped to reveal morphological features of the active part of the landslide, which were no longer visible on the ground during this geophysical survey. Combining the EMI results with the SP field a basic water regime mechanism within the landslide body could be determined. An experimental employment of

the gravity measurements and GRS accompanied with SRE brought new experience with the applicability of these methods. The Bouguer anomaly curve observed on profile K1 could serve as an additional constraint for the landslides spatial definition. In our case a clear gravity low depicts the position of the landslide body. We explain this phenomenon with the material disintegration within the landslide body, resulting in decreased density of the material.

The proposed combination of geophysical methods and cross-validated interpretation provides a more reliable geological model, which is crucial for information exchange with other geoscientific disciplines, especially for slope stability calculations and hazard assessment.

Acknowledgements. The authors are grateful to the Slovak Research and Development Agency APVV (grant No. APVV-0129-12) and the Slovak Grant Agency VEGA (grant Nos. 1/0131/14 and 1/0462/16) for the support of their research.

References

- Bárta J., Dostál D., Beneš V., Tesař M., 2005: Application of geophysical methods in the study of landslide movements, taking into account geological conditions in the sudety mountains. *Acta Geodyn. Geomater.*, **2**, 3, 121–129.
- Birch F. S., 1998: Imaging the water table by filtering self-potential profiles. *Ground Water*, **36**, 779–782.
- Bruno F., Marillier F., 2000: Test of High-resolution seismic reflection and other geophysical techniques on the boup landslide in the Swiss Alps. *Surveys in Geophysics*, **21**, 333–348.
- Čermák D., Varga M., 1999: Engineering-geological survey for individual housing construction – Pod Hradom Kapušany locality (IG prieskum pre IBV – lokalita Pod Hradom Kapušany). Manuscript, State Geological Institute of Dionýz Štúr, Bratislava, 10 p. (in Slovak).
- Corry E., 1985: Spontaneous polarization associated with porphyry sulfide mineralization. *Geophysics*, **50**, 1020–1034.
- Dahlin T., Bernstone C., Loke M. H., 2002: A 3-D resistivity investigation of a contaminated site at Lernacken, Sweden. *Geophysics*, **67**, 6, 1692–1700.
- Di Maio R., Mauriello P., Patella D., Petrillo Z., Piscitelli S., Siniscalchi A., 1998: Electric and electromagnetic outline of the Mount Somma-Vesuvius structural setting. *J. Volcanol. Geotherm. Res.*, **82**, 219–238.
- Dostál I., Putiška R., Kušnirák D., 2014: Determination of shear surface of landslides using electrical resistivity tomography. *Contributions to Geophysics and Geodesy*, **44**, 2, 133–147.

- Finizola A., Lénat J. F., Macedo O., Ramos D., Thouret J. C., Sortino F., 2004: Fluid circulation and structural discontinuities inside Misti volcano (Peru) inferred from self-potential measurements. *J. Volcanol. Geotherm. Res.*, **135**, 343–360.
- Gajdoš V., Rozimant K., Viskup J., Janotka V., Mojzeš A., 2002: The complex geophysical assessment of foundation soil. Proceedings of “Laboratory and Field Observations in Seismology and Engineering Geophysics”, Institute of Geonics of the AS CR, Ostrava, 213–217 (in Slovak).
- Goryainov N.-N., Matveev V.-S., Varlamov N.-M., 1988: Use of geophysical methods for landslide and mudflow investigations. *Landslides and Mudflows*, **1**, UNESCO, Moscow, 134–145.
- Grandjean G., Gourry J. C., Sanchez O., Bitri A., Garambois S., 2011: Structural study of the Ballandaz landslide (French Alps) using geophysical imagery. *Journal of Applied Geophysics*, **75**, 531–542.
- Grech J., 2010: Kapušany Pod hradom – Landslide 2010 (Kapušany Pod hradom – Zosuv 2010). Manuscript, State Geological Institute of Dionýz Štúr, Bratislava, 20 p. (in Slovak).
- Hungr O., Leroueil S., Picarelli L., 2014: The Varnes classification of landslide types, an update. *Landslides*, **11**, 167–194.
- Laffers F., Ilkanič A., Jasovská A., Antolová D., Kopecký M., Ondrášik M., 2012: Rescue procedure of the landslide emergency in the Kapušany village (Sanácia havarijného zosuvu v obci Kapušany). Manuscript, State Geological Institute of Dionýz Štúr, Bratislava, 40 p. (in Slovak).
- Lapenna V., Lorenzo P., Perrone A., Piscitelli S., Rizzo E., Sdao F., 2005: 2D electrical resistivity imaging of some complex landslides in the Lucanian Apennine chain, southern Italy. *Geophysics*, **70**, 3, B11–B18.
- Loke M. H., Barker R. D., 1996: Rapid least-squares inversion of apparent resistivity pseudosections by a quasi-Newton method. *Geophysical Prospecting*, **44**, 131–152.
- Lorne B., Perrier F., Avouac J. P., 1999: Streaming potential measurements: 1. Properties of the electrical double layer from crushed rock samples. *J. Geophys. Res.*, **104**, 17857–17877.
- Maineult A., Bernabé Y., Ackerer P., 2004: Electrical Response of Flow, Diffusion, and Advection in a Laboratory Sand Box. *Vadose Zone Journal*, **3**, 1180–1192.
- Mojzeš A., 2000a: The possibilities of characterization of physical state of rock massif from the point of soil radon emanometry. Proceedings of “Data nad Results Management in Seismology and Engineering Geophysics”. Institute of Geonics of the AS CR, Ostrava, 50–52.
- Mojzeš A., 2000b: The possibilities of evaluation of physical state of rock massif from the point of its radioactivity. Proceedings of 2nd Conference “Radioactivity in Environment”. Ministry of Environment of SR, Spišská Nová Ves, 112–114.
- Naudet V., Revil A., Rizzo E., Bottero J. Y., Bégassat P., 2004: Groundwater redox conditions and conductivity in a contaminant plume from geoelectrical investigations. *Hydrol. Earth Syst. Sci.*, **8**, 1, 8–22.
- Pellerin L., 2002: Applications of electrical and electromagnetic methods for environmental and geotechnical investigations. *Surveys in Geophysics*, **23**, 2-3, 101–132.

-
- Prokešová R. , Kardoš M., Tábořík P. , Medveďová A. , Stacke V., Chudý F., 2014: Kinematic behaviour of a large earthflow defined by surface displacement monitoring, DEM differencing, and ERT imaging. *Geomorphology*, **224**, 86–101.
- Ramola R. C., Choubey V. M., Negi M. S., Prasad Y., Prasad G., 2008: Radon occurrence in soil-gas and groundwater around an active landslide. *Radiation Measurements*, **43**, 98–101.
- Revil A., Pezard P. A., Glover P. W. J., 1999: Streaming potential in porous media: 1. Theory of the zeta potential. *J. Geophys. Res.*, **104**, 20021–20031.
- Reynolds J. M., 2011: *An Introduction to Applied and Environmental Geophysics*, John Wiley and Sons Ltd, Chichester, 712 p., second edition.
- Rizzo E., Suski B., Revil A., Straface S., Troisi S., 2004: Self-potential signals associated with pumping tests experiments. *J. Geophys. Res.*, **109**, B10203.
- Ruffell A., Wilson J., 1998: Near-surface Investigation of Ground Chemistry using Radiometric Measurements and Spectral Gamma-ray Data. *Archeological Prospection*, **5**, 203–215.